2018-01-0413 Published 03 Apr 2018

Modeling and Controls Development of 48 V Mild Hybrid Electric Vehicles

SoDuk Lee, Jeff Cherry, Michael Safoutin, Anthony Neam, Joseph McDonald, and Kevin Newman
U.S. Environmental Protection Agency

Citation: Lee, S., Cherry, J., Safoutin, M., Neam, A. et al., "Modeling and Controls Development of 48 V Mild Hybrid Electric Vehicles," SAE Technical Paper 2018-01-0413, 2018, doi:10.4271/2018-01-0413.

Abstract

The Advanced Light-Duty Powertrain and Hybrid Analysis tool (ALPHA) was created by EPA to evaluate the Greenhouse Gas (GHG) emissions of Light-Duty (LD) vehicles. ALPHA is a physics-based, forward-looking, full vehicle computer simulator capable of analyzing various vehicle types combined with different powertrain technologies. The ALPHA desktop application was developed using MATLAB/Simulink. The ALPHA tool was used to evaluate technology effectiveness and off-cycle technologies such as air-conditioning, electrical load reduction technology and road load reduction technologies of conventional, non-hybrid vehicles for the Midterm Evaluation of the 2017-2025 LD GHG rule by the U.S. Environmental Protection Agency (EPA) Office of Transportation and Air Quality (OTAQ). This paper presents controls development, modeling results, and model validation for simulations of a vehicle with a 48 V Belt Integrated Starter Generator (BISG) mild hybrid electric vehicle and an initial model design for a 48 V inline on-axis P2-configuration mild hybrid electric vehicle. Both configurations were modeled with a MATLAB/Simulink/Stateflow tool, which has been integrated into EPA's ALPHA vehicle model and was also used to model components within Gamma Technology GT-DRIVE simulations. The mild hybrid electric vehicle model was validated using vehicle data obtained from Argonne National Laboratory (ANL) chassis dynamometer tests of a 2013 Chevrolet Malibu Eco 115 V 15 kW BISG mild hybrid electric vehicle. The simulated fuel economy, engine torque/speed, motor torque/speed, engine on-off controls, battery voltage, current, and State of Charge (SOC) were all in good agreement with the vehicle test data on a number of drive schedules. The developed 48 V mild hybrid electric vehicle model can be used to estimate the GHG emissions and fuel economy of 48 V mild hybrid electric vehicles over the EPA regulatory drive cycles and to estimate off-cycle GHG emissions. The 48 V mild hybrid electric vehicle model will be further validated with additional 48 V mild hybrid electric vehicle test data in the future as more vehicle models become available. EPA has included 48 V BISG mild hybrid electric vehicle technology in its assessment of CO2-reducing technologies available for compliance with U.S. GHG standards.

Introduction

The Advanced Light-Duty Powertrain and Hybrid Analysis (ALPHA) tool was developed by EPA to model vehicle performance, fuel economy, greenhouse gas (GHG) emissions and battery pack performance for light-duty conventional and hybrid electric vehicles (HEV). The ALPHA model can be used as a support tool for the development of future GHG emissions regulations and as a research tool to evaluate the efficiency of new advanced technologies. The ALPHA [1, 2] hybrid model is related to the heavy-duty vehicle Greenhouse Gas Emissions Model (GEM) currently used for determining GHG emissions compliance for heavy-duty vehicle applications in the U.S. [3]. The basic model strategies and controls within GEM (with the exceptions of specific traction motor, generator, battery, regenerative braking control, hybrid vehicle supervisory control, etc.) can be used within ALPHA for modeling light-duty HEV applications.

Relative positioning of electric machines for HEVs are shown schematically in Figure 1. This positioning includes

FIGURE 1 Schematic representation of the relative electric machine positioning (P_i) for different hybrid electric vehicle architectures

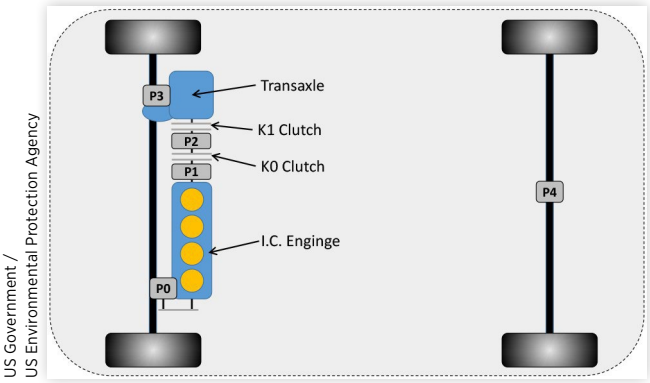

P0 (direct coupling to the engine front accessory drive), P1 (direct coupling to engine crankshaft power output), P2 (positioned between the engine and transmission or transaxle with clutch isolation), P3 (coupled to a front differential), and P4 (coupled to a rear differential). Mild hybrid electric vehicles (MHEVs) typically use working voltages at or below 150 V DC. Limiting MHEV voltage to below 60 V DC (e.g., 48 V MHEV) can potentially reduce the cost, complexity, and weight of systems necessary to comply with U.S. motor vehicle safety regulations [4] while potentially maintaining effectiveness comparable to higher voltage systems for reducing GHG emissions.

Both 48 V Belt Integrated Starter Generator (BISG) P0 and 48 V P2 MHEV models were developed to estimate vehicle performance, fuel economy and GHG emissions. Development of the P2 vehicle model shares many characteristics with development of the P0 model and details of models for both MHEV types are presented in this paper. Modeling and validation results are shown only for the P0 MHEV in this paper due to the availability of P0 MHEV chassis dynamometer data from a production vehicle application. Modeling and validation results for the 48 V P2 MHEV will be presented separately in the near future pending the availability of P2 HEV vehicle-level and component-level chassis dynamometer data.

The vehicle supervisory controls (VSC), battery power limits and battery state of charge (SOC) controls for both the P0 and P2 MHEV models were initially prototyped and developed using the Gamma Technologies, LLC (Westmont, IL) GT-DRIVE™ vehicle model with the addition of dynamic link libraries (DLLs) developed using Microsoft Visual Studio. The MATLAB/Simulink- and Stateflow-based control strategies and algorithms within the DLLs were also easily ported for eventual use within the EPA's ALPHA vehicle electrification model.

The battery and engine DLLs were created directly from the same module used within the ALPHA vehicle model and can be used either in ALPHA or GT-DRIVE. A 48 V VSC DLL was developed to model P0 48 V MHEVs. Previously developed P2 strong HEV control strategies [5] were used to model the 48 V P2 MHEVs since the hybrid electric vehicle systems, motor, power coupling, engine plant models and controls for the inline P2 48 V MHEVs and P2 strong HEVs have similar launch and regeneration power and also similar battery pack energy (kWh) capacity. A lithium-ion (Li-ion) battery pack model was used for simulation of both the P0 and P2 MHEVs. The battery pack model [6, 7, 8] contains a two-time constant equivalent circuit battery cell model, a lumped capacitance battery thermal model and battery management system (BMS) thermal control strategies. Initial model development and validation reported in this paper were conducted using GT-DRIVE, but the DLLs and modeling strategies have been ported into ALPHA for use in future EPA MHEV analyses. GT-DRIVE MHEV model validation was conducted by comparison of vehicle and component simulation results with vehicle-level and component-level results generated during chassis dynamometer testing of a P0 MHEV over EPA regulatory cycles.

Vehicle Model

In this section, the hybrid electric vehicle model is described in terms of its overall architecture/structure and each of the component models. The HEV model is a forward-looking vehicle model which represents light-duty (LD) HEVs. The current version simulates vehicles with a fully warmed-up engine, with a base conventional powertrain, and with either P0 or P2 electric machine positioning.

Model Architecture

Both the commercial GT-DRIVE and EPA ALPHA HEV models consist of a user-friendly Graphical User Interface (GUI) and the underlying component models. The dynamic linked libraries (DLLs) used within the GT-DRIVE vehicle model are written within the MATLAB/Simulink/Stateflow environment. The GT-DRIVE and ALPHA generic GUIs can be used to setup light-duty and light-heavy-duty conventional and hybrid vehicle Design of Experiments (DOE) to estimate drive cycle GHG emissions, are capable of generating response surface model inputs for specific technology combinations, and also provide easy access for end-user input into the models. The compatibility of DLL's between both models allowed initial model and control system prototyping development to be conducted within the GT-DRIVE environment with eventual porting of modeling and control strategies into EPA's ALPHA model.

The base architecture of the HEV model consists of three layers: Systems, Components, and Functions. There are six plant model and control systems (Driver, Electric Motor, Battery, Engine, Transmission, and Vehicle) and VSC. The ALPHA battery and engine modules were compiled using Microsoft Visual Studio 10 and the MATLAB/Simulink (version 2016a) to create GT-DRIVE (version 2018) DLLs to precisely control and represent various engine states, battery power limits, battery SOC, battery charging efficiencies, etc. Some of the systems (e.g. Electrical, Engine, Transmission, and Vehicle) consist of components, each of which represents a physical entity that, when combined, make up the entire system. Functions are mathematical equations that represent the systems and/or components.

TABLE 1 Overall Structure of 48 V MHEV System Model

Systems	Components
Driver and Ambient	N/A
Engine	Internal Combustion Engine, Mechanical Accessories
Power-Coupling & Transmission	Automatic Transmission, Clutches
Electric Machine	Electric Machine, DC-DC Converter, Inverter, Electrical Accessories
Battery	Li-ion battery and BMS
Vehicle	Final Drive, Drive Axle, Tires, Chassis
VSC	Engine On/Off, Motor Power, Battery Management System

System Models

In this section, brief descriptions for each of the systems are provided. These system models remain consistent regardless of vehicle types and classes, in other words whether the vehicle is a P0 or P2 HEV. The ambient conditions, significant portions of driver interactions, engines, chassis, and conventional transmissions all share common system models. Therefore, these common system models will not be presented within this paper.

Engine Most of the previously published engine system models in [1, 2] can be used for hybrid electric vehicle applications by simply updating to include the engine operational maps, such as from a gasoline direct injection (GDI) or an Atkinson cycle port fuel injection (PFI) engine, and by eliminating some portion of the engine controls and operating modes, e.g. idle speed control and idle operation.

A 2.5 L GDI engine map was previously developed for ALPHA modeling based upon engine dynamometer testing of a 2013 GM Chevrolet Malibu 1LS [2]. For MHEV modeling, the 2.5 L GDI map was used in order to create a surrogate fuel map [9] for the engine used by 2013 GM Chevrolet Malibu Eco modeled within this study. The surrogate BSFC map shown in Figure 2 was then used to develop models of both P0 and P2 48 V MHEVs.

FIGURE 2 2013 GM Malibu EcoTec Engine Brake Specific Fuel Consumption (BSFC, top) and Brake Thermal Efficiency (BTE, bottom) Maps

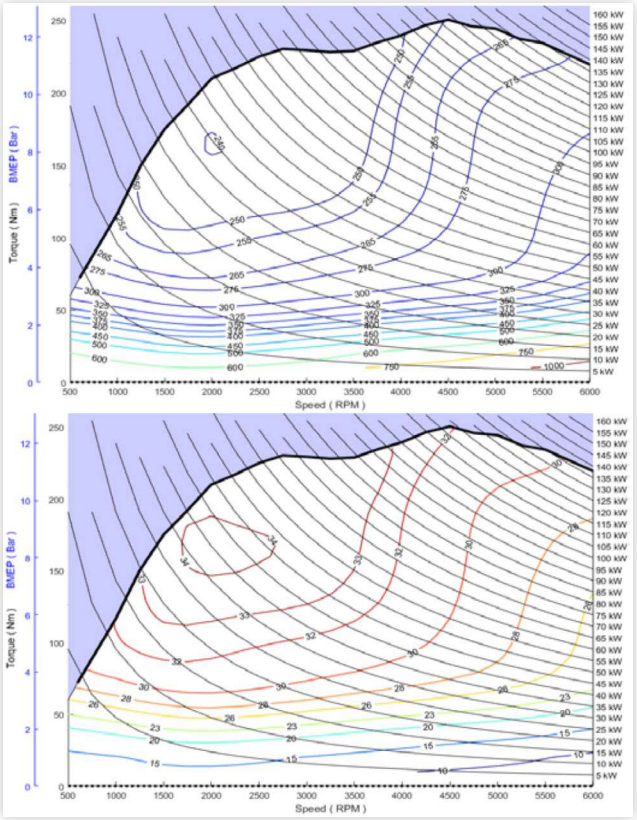

Power-Coupling and Transmission The P0 and P2 MHEVs have different power transfer mechanisms when combining engine power and motor electric power. The regenerative brake energy recovery, belt-drive transmission losses, and engine inertial power losses due to the direct, belt-drive engine/motor coupling used by P0 MHEVs resulted in more energy losses when recuperating the brake energy and during electric motor power transmission compared to the P2 MHEVs due to the inability of the P0 configuration to operate the electric machine completely independently from the engine. Therefore, different P0 and P2 hybrid power-coupling and energy flow controls and GM 6 T40 6-speed automatic transmission models are used by ALPHA and were incorporated into the hybrid electric vehicle model by using a variant sub-system to represent P0 or P2 configurations within the MATLAB/Simulink environment.

Po System Description The modeled components of the P0 MHEV system are summarized in Figure 3. A small 12/15 kW electric machine is directly mounted to the engine front accessory drive system by a seven-groove belt-pulley. The tractive power free energy of the vehicle available during deceleration is transferred to the electric machine and is used to charge the 48 V Li-ion battery even if the engine shuts off during deceleration. However, there are energy losses during the regenerative brake energy recovery process so that the available energy has to be reduced by engine inertia, engine friction, inverter losses, and belt-pulley system losses. The power transmission efficiency of a seven-groove belt-pulley drive is less than typical gear and clutch efficiencies for P2 systems. Typical published efficiencies for a multi-groove belt-pulley [9] were used to model 48 V P0 MHEVs. The power available during P0 regenerative braking was calculated from the motor/generator efficiency and the regenerative charging power as shown in the Eq. (3).

The DC electric power used to charge the 48 V battery pack is converted by an inverter from the AC power generated by the P0 electric machine. The battery pack may enable limited electric-only vehicle driving capability similar to a P2 MHEV system when the demanded vehicle tractive power is less than the available battery discharge power limit at very

FIGURE 3 12/15 kW 48 V BISG P0 MHEV Model Components

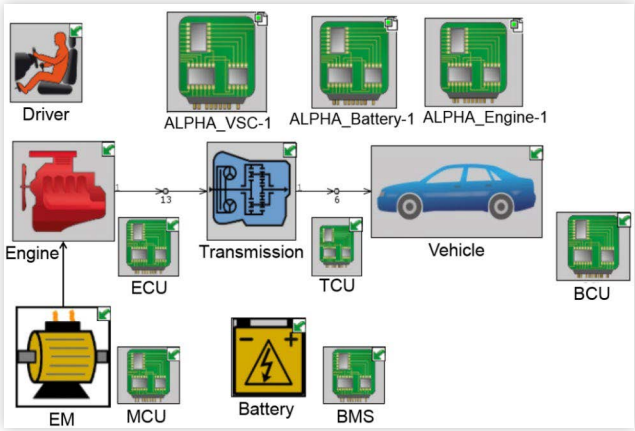

low vehicle speeds (e.g., parking maneuvers and vehicle creep in heavy traffic). The P0 system can be mathematically described in the following manner:

$$T_{coupler} = T_{engine} + T_{BISG} \cdot r_{BISG} \cdot \beta_{eff} \quad (1)$$

$$T_{loss} = T_{FMEP} + T_{inertia} = T_{FMEP} + I\frac{d\omega}{dt} \quad (2)$$

$$P_{eng\_on} = T_{coupler} \cdot \omega, P_{eng\_off\_rgen} = \varphi \cdot P_{tractive} + T_{loss}\,\omega \quad (3)$$

where, r_{BISG} is the belt-pulley ratios of the BISG electric machine. $\beta_{eff}, \omega, I, and \frac{d\omega}{dt}$ are the belt power/torque transmission efficiency, engine speed, the moment of engine inertia, and engine angular acceleration, respectively. T_{engine}, T_{BISG}, and T_{FMEP} are torque from the engine, from the BISG and engine friction torque, respectively, P_{eng_on} is the power during the engine on-state, $P_{eng\_off\_rgen}$ is the regenerative power during the engine-off state. An empirical regenerative brake energy recuperation efficiency, φ, was used to validate the regenerative braking energy recuperation of both the P0 and P2 48 V MHEVs. The negative portion of vehicle tractive power ($P_{tractive}$) multiplied by the regenerative braking energy efficiency and the positive friction and engine inertia torque losses (T_{loss}) were added to estimate the electric power applied to the BISG motor for P0 applications. The regenerative brake power, P_{rgen_brake}, [11, 12] of the BISG is calculated by using 48 V motor/generator efficiency maps as shown in Eq. (4):

$$P_{rgen\_brake} = P_{eng\_off\_rgen} \cdot \psi \quad (4)$$

where, ψ is the BISG efficiency. Development of the motor efficiency maps is described in a subsequent section of this paper.

P2 System Description The P2 MHEV has a combination of a single traction motor/generator, a gear box and a clutch. The clutch allows independent operation of the electric machine by allowing it to completely decouple from the engine and transmission.

The engine and motor torque in a parallel HEV system can be estimated by equation (5). The driveline shaft torque is calculated by multiplying the final drive gear ratio to the clutch output shaft torque shown in equation (6).

$$T_{coupler} = T_{engine} + T_{motor} \quad (5)$$

$$T_{driveline} = T_{coupler} * r_{Gear}(\text{gear position}) * g_{fdr} \quad (6)$$

where, $T_{coupler}$, T_{engine}, and T_{motor} are torque from the torque coupler, engine, and traction motor, respectively. The r_{Gear} term is the gear ratio of the selected gear position, and g_{fdr} is the final drive gear ratio.

The approximately 80% efficiency for regenerative brake energy recovery of the P2 system is significantly higher than the approximately 50% efficiency of the P0 system since the K0 clutch (Figure 1) between the engine and electric machine of the P2 system can be disengaged during vehicle deceleration to isolate the losses such as those caused by engine friction and, engine inertial forces [13].

Battery Pack An A123 Systems 0.4kWh 48 V 14S1P Li-ion battery pack was tested at the U.S. EPA National Vehicle and Fuel Emissions Laboratory (NVFEL) battery testing laboratory using battery pulse tests to characterize the ohmic short/long-time resistance and capacitance. The tests were conducted using 10 second discharging and charging pulse currents to measure the parameters necessary to develop an initial model of the 48 V Li-ion battery pack's electrical characteristics. A detailed description of development of the 48 V battery pack model has been published within a related paper [14]. The tested and modeled pack design uses a proprietary Li-ion pouch cell design. This 48 V battery pack design was the basis for all of the 48 V MHEV simulations in this study. The 2013 Malibu Eco mid-size MHEV was originally equipped with a somewhat higher capacity and higher voltage battery pack. The vehicle used a 0.5kWh, 4.4 Ah, 32 cell, 115 V Li-ion battery pack. The recently introduced 2018 Buick Lacrosse eAssist mid-size car is equipped with a 0.45kWh, 24 cell, 86 V Li-ion battery pack that has been repackaged more compactly and yet can store a level of regenerative braking energy comparable to the older Malibu Eco pack. The compact packaging of the newer GM 0.45kWh battery pack design has also allowed it to be located under the center console in the 2016 GM Silverado 1500 eAssist light-duty pickup truck application.

The battery model contains an equivalent circuit cell model, a lumped capacitance battery thermal model, and Battery Management System (BMS) controls. The MATLAB/Simulink-based equivalent circuit battery model was implemented in both EPA's ALPHA vehicle model and Gamma Technology GT-DRIVE vehicle model using Microsoft Visual Studio DLLs [14].

As shown in Figure 4, both the discharge and charge power limits were reduced to zero when the battery pack temperature rises to above 65 °C or falls below −30 °C, which represents the upper and lower operating temperature limits, respectively, for this particular Li-ion cell chemistry. The desired operating temperature of the modeled 48 V Li-ion battery is between 20 and 55 °C although a limited battery operating mode can be extended between −30 and 65 °C.

FIGURE 4 The Power Limits of a 48 V Li-ion Battery Pack

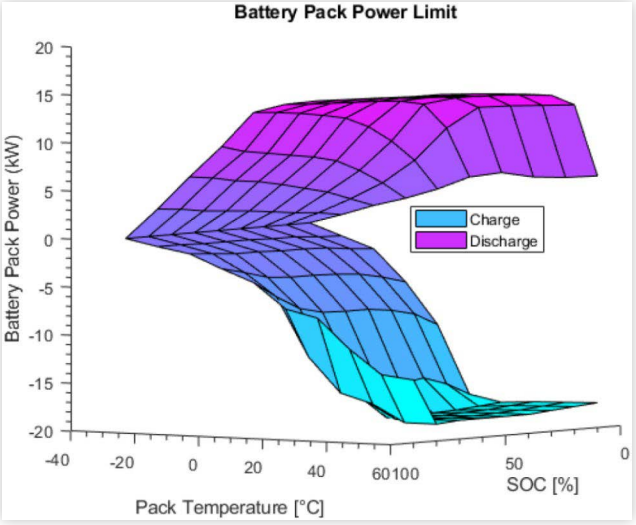

US Government / US Environmental Protection Agency

The maximum allowable charging and discharging power limits of the 48 V battery pack are 16 kW and 15 kW respectively at 50% SOC, 25 °C battery pack temperature, and near the beginning-of-life of the battery pack. The BMS has self-balancing SOC control functionality. At −30 °C temperature, the modeled 48 V battery pack can still discharge approximately 30A for 10 seconds at 50% SOC, which is sufficient to crank the engine during cold start. The 10 second discharging and charging current limits are approximately 370A at between 30% SOC and 60% SOC, and between 30 and 60 °C battery pack temperature.

The battery charge and discharge power was derived from ANL chassis dynamometer data of the 2013 Chevrolet Malibu Eco 115 V MHEV over regulatory drive cycles [15, 16] and was applied to the A123 Systems 48 V Li-ion battery pack for laboratory testing using a hardware-in-the-loop configuration [14]. As shown in the first plot of Figure 5, the battery pack can maintain acceptable voltage levels between 40 and 50 V at a root-mean-square (RMS) current of 47.2A over the Urban Dynamometer Driving Schedule (UDDS). The modeled 46.2 V RMS battery pack voltages were in excellent agreement with the 46.01 V RMS battery pack voltages measured during hardware-in-the-loop (HIL) testing over simulated UDDS operation [14].

Figure 6 shows that the modeled and measured SOC during HIL testing were in good agreement. The "tooth-shaped" measured SOC was due to 20 Hz/50 ms battery BMS CAN transmission rate updates. The 48 V Li-ion battery pack model calculated reasonable battery pack voltages, SOC, and pack temperatures while satisfying the requirements of discharging and charging power and current limits at the estimated battery pack temperatures and SOC levels. A more detailed description of the 48 V Li-ion battery pack testing and modeling along with battery model validation results is presented elsewhere [14].

Electric Machine Torque and Efficiency Maps Efficiency relative to speed and torque of the 8.5 kW electric machine used by the 2011 Sonata HEV was evaluated by Oak Ridge National Laboratory (ORNL) [17]. EPA scaled this motor efficiency map to estimate both 12 kW launch assist and 15 kW regenerative energy charging. The scaled efficiency map was then compared to a proprietary 12/15 kW 48 V electric machine efficiency map provided to EPA by a Tier 1 automotive supplier and initial GT-DRIVE simulations were conducted to compare estimated UDDS and Highway Fuel Economy Test (HwFET) fuel economy and GHG emissions between the scaled and proprietary maps. The simulated fuel economy and GHG emissions showed negligible differences between using the scaled versus the proprietary efficiency maps. Therefore, the scaled electric machine efficiency map based upon the published data from ORNL was used to model the 48 V electric machines included in this study. The resulting scaled 4-quadrant motor power and efficiency map for the P0 48 V MHEV model is shown in Figure 7.

FIGURE 5 Voltage and Temperatures of a 48 V Li-ion Battery Pack

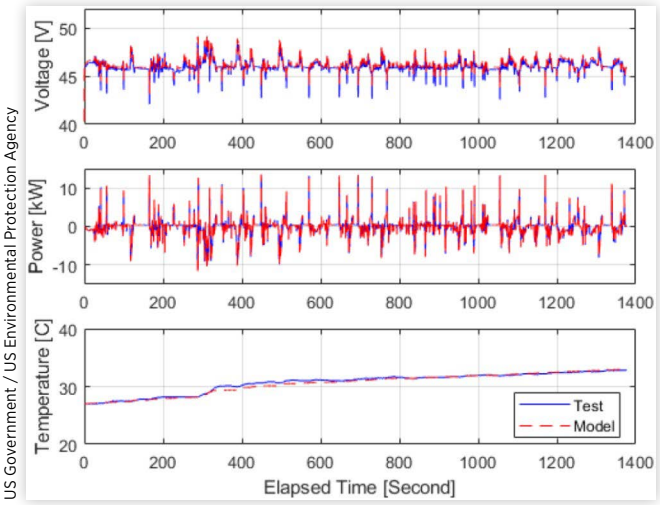

FIGURE 6 SOC Simulations of a 48 V Li-ion Battery at UDDS

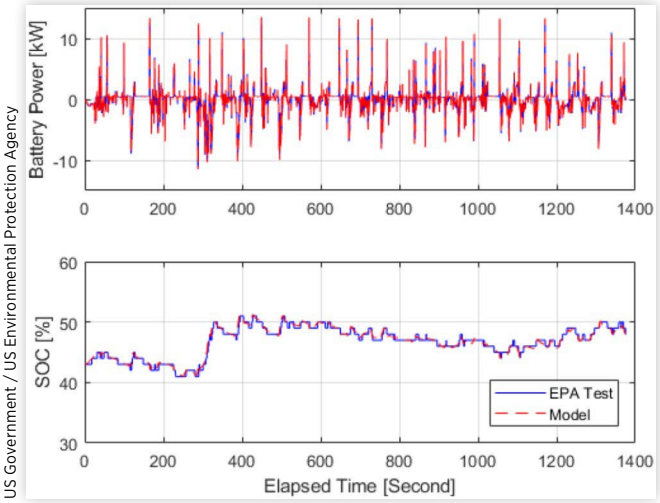

FIGURE 7 A Four-Quadrant 48 V BISG Motor Efficiency Map Derived via Scaling of Publicly Available Data (an enlarged version of this figure is also shown in Appendix Figure 1)

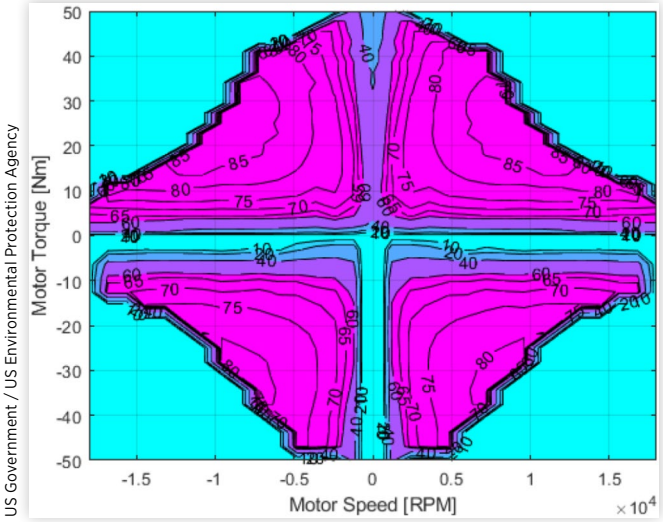

Electric machine torque from model simulations was compared with ANL chassis dynamometer vehicle test data since discharge current is heavily dependent upon traction motor torque demand. The simulated motor torque was in good agreement with motor torque calculated from the vehicle test data [16]. The motor currents were calculated using the following relationship:

$$I_m = \frac{\left(T_{motor}\,\omega_m\right)}{V_{Batt}}\eta_{\text{eff}} = \frac{P_{motor}}{V_{Batt}} \tag{9}$$

where the subscript m is the P0 or P2 motor, the subscript *Batt* represents battery, ω is motor angular speed, η_{eff} is motor efficiency, P is power, and T is torque. By supplying the demanded motor torque and speed generated by the vehicle supervisory controller, the motor current was calculated by dividing the battery pack voltage from the battery power estimated using a two-dimensional look-up table.

Hybrid Vehicle Supervisory Controls

Engine ON and Torque Control A 10 second discharge power limit for the Li-ion battery pack was used to estimate the available Discharge Power Limit (DPL) by subtracting the discharge power at the minimum SOC from the discharge power at the current SOC as shown in equation (10).

$$DPL_{avail} = DPL\left(SOC(t)\right) - DPL\left(minimum\,SOC\right) \tag{10}$$

A 30% SOC was used as a typical default minimum SOC. The engine can be turned off when the sum of the demanded road load power and the accessory electric power is less than the available discharge power limit since the traction motor can be designed to provide sufficient electric-only propulsion at low vehicle speeds for a P2 configuration or under more limited conditions for a P0.

Engine power required is calculated by subtracting the battery pack power from the sum of the road-load power and the accessory electric power as shown in equation (11):

$$P_{engine} = P_{road\_load} + P_{acc} - P_{batt}$$
$$T_{engine} = \frac{P_{engine}}{\left(\omega_e\right)} \tag{11}$$

where ω_e is engine speed in radians per second. The road-load power contains the driveline system losses, gear efficiency losses, aerodynamic drag, tire friction, etc.

The VSC was developed primarily to calculate electric motor activation timing, the required torques from the motor/generator, and the demanded engine torque. The battery power is discharged to provide the demanded electric motor torque when the pedal acceleration is greater than a defined pedal acceleration or engine load threshold while the vehicle tractive power is greater than zero. Various threshold values were stored in two-dimensional lookup tables as functions of engine speed and vehicle speed since an engine might be operating more efficiently at somewhat higher vehicle speed, depending on the transmission gear selected and road load forces encountered (aerodynamic drag, rolling resistance, etc.). The electric motor discharge power, EM_{pwr_dmd}, is dependent on the battery discharge power limits (P_{batt}):

$$EM_{pwr\_dmd} = \min\left(P_{batt}, EM_{peak\_pwr}\right).Pedal_{accel} \,/\, threshold \tag{12}$$

The battery discharge power limits depend on the pack temperature, SOC level, battery aging, etc. The battery SOC was controlled by the overall energy flows, and therefore total energy flows of the model simulations and the ANL vehicle test data were in good agreement, although the modeled SOC does not mimic the tested SOC profiles on a second-by-second basis (Figure 8). Rule-based controls [18, 19] were then used to further refine the engine speeds, engine power and motor/generator power to operate the engine closer to high efficiency points of operation while satisfying the demanded vehicle tractive power requirements. The same engine power can be obtained by controlling engine speeds and transmission gear selection around the area of the high efficiency (sometimes referred to as the "sweet spot") of engine speed vs. torque. Detailed development of the rule-based VSC systems is beyond the scope of this paper, and will be presented separately in the future.

As shown in Figure 9, the engine is turned on if the demanded road-load power is greater than the available battery pack discharge power limit. However, the engine is operated near a high-efficiency region of engine speed and torque to minimize fuel consumption and CO_2 emissions as shown in Figures 8 and 9. Any excess engine power is used to charge the battery pack.

Figure 9 shows a total of 1071 seconds of engine-on time from the model simulation of the UDDS, which is in an excellent agreement with the 1070 seconds of engine-on time from ANL chassis dynamometer test data of the 2013 Chevrolet Malibu Eco over the UDDS. Thus, the simulated engine-on time was comparable to vehicle test data when the available battery discharge power limits were maintained.

FIGURE 8 Engine Power Near Minimum BSFC Modeled for 2.5 L GM Ecotec Engine Compared to Chassis Dynamometer Test Data of Engine Power and Road Load (top) Along with the Resulting Measured (red) and Modeled (blue) SOC (bottom) for Phase 1 (initial 505 s) of the UDDS.

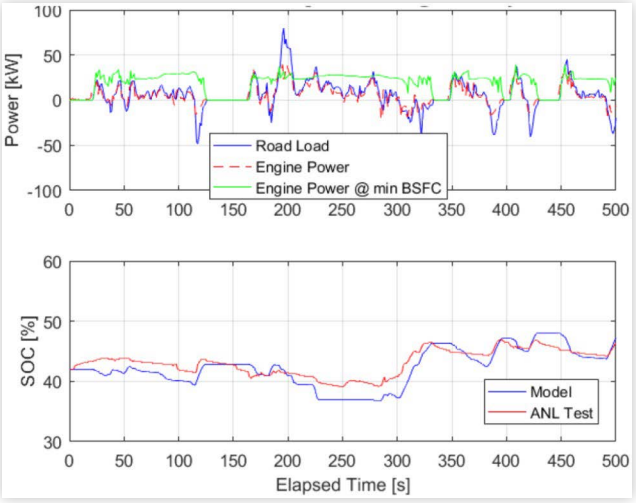

FIGURE 9 Measured (red) and Modeled (blue) Engine Speed and Engine-ON State of 2013 GM Malibu Eco for the UDDS (1 is Engine-ON, 0 is Engine-OFF).

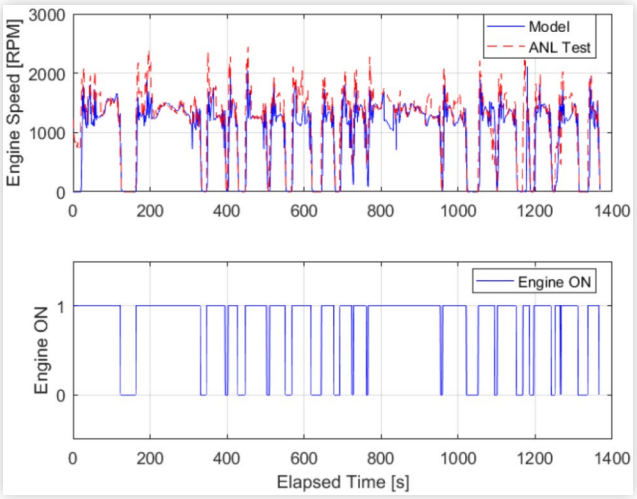

FIGURE 10 Vehicle Tractive Power, Engine Torque and SOC Simulations (blue) Compared to Chassis Dynamometer Test Data (red) Over the UDDS.

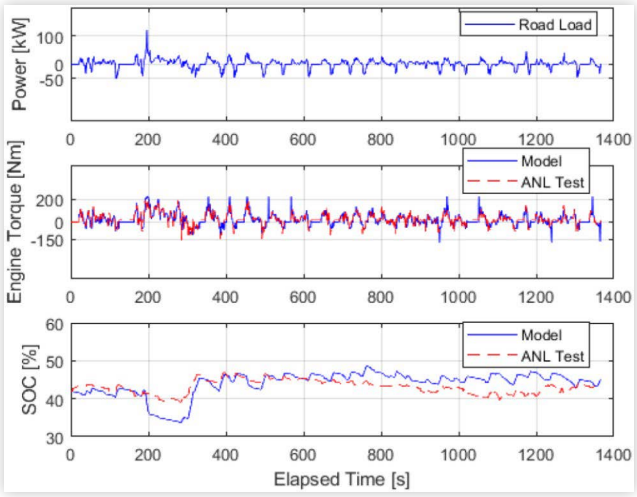

The engine torque error, *e(t)* in equation (13), is obtained by subtracting actual vehicle speed from the specified drive cycle vehicle speed. A generic PID controller shown in equation 13 can be used to estimate an optimum engine torque to follow the demanded drive cycle vehicle speed during engine-ON driving.

$$T_{\text{engine}} = K_p\, e(t) + K_I \int e(t)\,dt + K_D \frac{d}{dt} e(t)\,dt$$
$$K_P = 5.23, K_I = 0.01, K_D = 0.021 \quad (13)$$

For the initial and final values of SOC balancing, the following PID controller was implemented to compensate battery power in order to rapidly control the final SOC values to be closer to the initial SOC value as shown in the third plot in Figure 10. The SOC "swing windows" of the 0.4kWh 48 V battery pack were greater than the SOC "swing windows" of the production 0.5kWh 115 V 2013 Malibu Eco battery pack since SOC varies more quickly from the somewhat smaller capacity 48 V battery pack when charging and discharging using a similar magnitude of electric power. SOC is represented in the model in the following manner:

$$\Delta Power_{Batt} = \text{PL}\left(\text{SOC}(t)\right) - \text{PL}\left(SOC_{target}\right)$$
$$Power_{comp} = \Delta Power_{Batt} + k_P\, \Delta SOC(t) + k_I \int \Delta SOC(t)\,d(t) + k_D \frac{d}{dt} \Delta SOC(t)\,d(t)$$
$$\Delta SOC(t) = \text{SOC}(t) - SOC_{target},$$
$$k_P = 15.7, k_I = 3.5, k_D = 0.018 \quad (14)$$

where *PL* is the discharge and charge power limit for positive and for negative current. The battery power difference, $\Delta Power_{Batt}$, is estimated by subtracting the power limit at the SOC target from the power limit at a current SOC level. The $Power_{Batt}$ for compensating ΔSOC(t) must be limited to operation within the available battery discharging and charging power limits.

Motor Torque and Running-Time Control The traction motor torque in the 48 V parallel MHEV simulations was estimated by subtracting engine torque from the demanded driver torque:

$$T_{motor\_est} = min\left(T_{mot\_max}, \left(T_{trac} / g_{fdr} - T_{engine}.r_g\right) / r_g\right) \quad (15)$$

where T is torque, g_{fdr} is the final drive gear ratio, r_g is the transmission gear ratio, T_{trac} is the driver demanded torque/vehicle tractive torque, and T_{mot_max} is the maximum allowable motor torque estimated by the minimum values of the discharge/charge power limits of the battery pack and motor peak power. Finally, the motor torque, T_{motor}, is calculated by using the pulley ratios of the P0 electric machine or the speed gear reduction ratios in the case of a P2 electric machine.

As shown in Figure 11, motor power is provided in addition to the engine power required to propel the vehicle to assist with vehicle launching. The peak motor power is limited for the first 10 seconds, and reduced to normal motor power levels afterwards. The motor runs for approximately 3~5 seconds to meet the demanded driver torque quickly before reaching approximately 1200~1500 RPM, which is near a high efficiency region of engine speed vs. torque. The motor torque is gradually reduced to conserve battery power after the engine provides sufficient torque to propel the vehicle. Also, the battery is charged by excessive engine power while running the engine more efficiently. The smaller negative charging power to the battery pack is reduced by engine friction power, engine inertia and motor efficiency converted from mechanical power to electrical power. To rapidly balance the final SOC values to the initial SOC values, the electric machine run time at launch is controlled adaptively as described in the next section.

FIGURE 11 Battery and Engine Power Simulation of a P0 48 V MHEV Over the Initial 200 Seconds of the UDDS

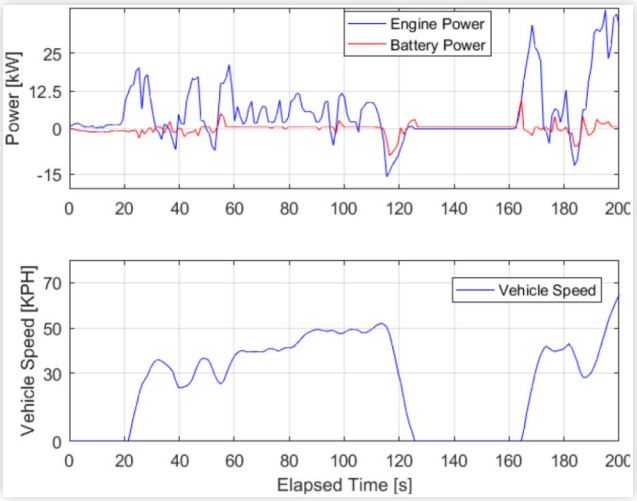

US Government / US Environmental Protection Agency

FIGURE 12 Measured (red) and Modeled (blue) SOC Trajectory of 2013 Malibu Eco over the UDDS

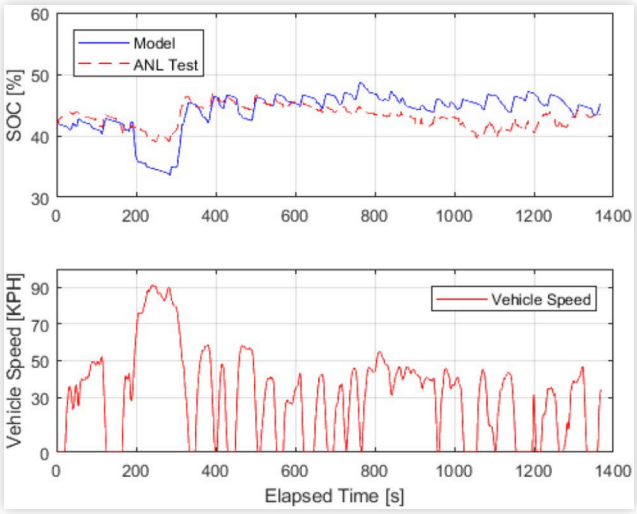

US Government / US Environmental Protection Agency

SOC Trajectory and Balancing Control As shown in Figure 12, the SOC trace trajectories from the model and ANL vehicle test data over the UDDS are similar even though the initial SOC values are different. The SOC trajectory surface can be constructed by various optimization schemes, but the optimization processes are computationally intensive. Therefore, a delta SOC compensation from vehicle test data and a PID controller were implemented to emulate typical hybrid electric vehicle SOC traces for the vehicle model simulations.

Validation and Simulation

Table 2 shows the target road load coefficients used for chassis dynamometer testing of the 2013 GM Chevrolet Malibu and the 2013 Malibu Eco MHEV. Road load coefficients for a conventional (non-MHEV/Eco) version of the 2013 Malibu are shown for comparison. The same 2013 Malibu Eco road-load coefficients were also used when modeling the Malibu Eco-based 48 V MHEV. The ANL test results were used to develop models of 48 V P0 and P2 MHEVs and to validate the P0 MHEV model. Other test and model parameters were obtained from ANL as well as from the published specifications of the vehicle's manufacturer.

The GT-DRIVE vehicle model was used by EPA for 48 V MHEV model development at an early conceptual stage. A visual schematic of the GT-DRIVE model is shown in figure 13. The EPA's engine and battery sub-models were compiled by Microsoft Visual Studio 10 using the 2016a version of the MATLAB/Simulink/Stateflow toolbox to create DLLs representing these components and were used as components within the GT-DRIVE model during model development. The ALPHA battery DLL was especially useful to precisely control the battery discharge and charge power limits, battery charging efficiency, pack temperature, etc., within GT-DRIVE. Detailed modeling of battery power is critical to properly

TABLE 2 Chassis Dynamometer A, B, C coefficients for the standard and MHEV "Eco" version of the 2013 Chevrolet Malibu.

Vehicle Model Year	Chassis Dynamometer Road-Load Coefficients	
2013 Chevrolet Malibu	A	169.3883 N
	B	2.3595 N/ (m/s)
	C	0.4092 N/(m/s)^2
2013 Chevrolet Malibu Eco	A	135.24146 N
	B	2.6976488 N/ (m/s)
	C	0.3213237 N/(m/s)^2

US Government / US Environmental Protection Agency

FIGURE 13 Schematic representation of GT-DRIVE Engine State and ALPHA Engine Model DLLs (an enlarged version of this figure is also shown in Appendix Figure 2)

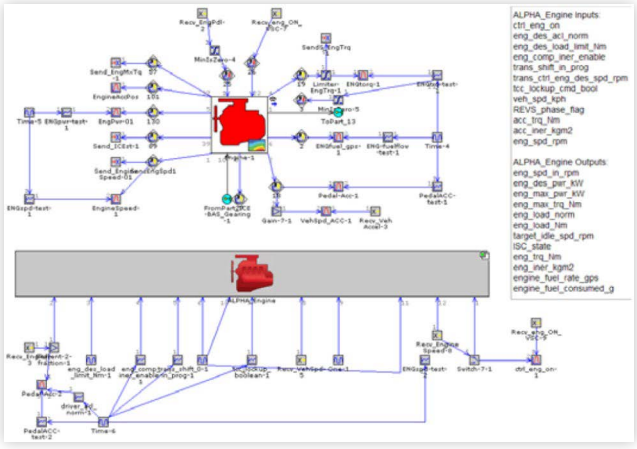

US Government / US Environmental Protection Agency

represent any vehicle electrification and resultant changes in fuel consumption and GHG emissions. The MHEV DLLs and control strategies developed in GT-DRIVER will eventually be ported back into the EPA ALPHA model.

UDDS Simulations of 48 V P0 MHEV Model

As shown in Figure 14, the simulated engine torque was operated near a region of high efficiency for the engine to minimize fuel consumption and CO_2 emissions. The trends of simulated engine torque and speed were in good agreement with the trends of the ANL chassis dynamometer test data. The simulated 57.1 Nm RMS engine torque for the 48 V P0 MHEV is within 4.5% of the 54.7 Nm RMS torque for the ANL vehicle test data [16]. Overall, the simulated engine torque and speed (Figure 14) were in good agreement with the chassis dynamometer test data.

The gear position shown in Figure 15 was estimated based upon driver pedal acceleration and transmission/vehicle speed. The transmission gear selection during the model simulations was in an excellent agreement with the transmission gears selected during chassis dynamometer testing.

The traction motor speed was determined by using vehicle speed, final drive ratio, tire radius, and speed reduction gear ratio (including torque convertor lock/unlock condition). The motor speed can be estimated by simple algebraic equations. An accurate estimation of traction motor torque is critical since the demanded motor torque and speed are used as inputs to the motor power maps to provide an estimate of battery current. The 1.99 kW RMS battery charge power modeled at 48 V was comparable to 1.99 kW RMS battery charge power from the 115 V Malibu Eco test data [16]. Overall, the simulated battery power and motor speed of 48 V P0 MHEV shown in Figure 16 agreed well with the battery power and motor speed measured during chassis dynamometer testing of the 115 V Malibu Eco.

The estimated motor current and accessory current were used as inputs into the model of the battery pack to estimate the resulting battery pack SOC and voltage. Charge/discharge efficiencies and battery pack temperature were also taken into account when estimating the battery pack SOC. The simulated 42.7A RMS current for the 48 V P0 MHEV was significantly higher than the 17.9A RMS from the 115 V MHEV vehicle test data over the UDDS due to the lower battery pack voltage and system voltage for the modeled 48 V system relative to the tested 115 V system. As shown in Figure 17, the simulated final SOC of the 48 V battery pack had lower discharged battery power and higher final SOC over the UDDS compared to the production 115 V Malibu Eco battery pack used during vehicle testing, and thus the modeled fuel economy results for the 48 V P0 MHEV represent a conservative estimation over the UDDS as shown in Table 3.

FIGURE 14 Comparison of Engine Torque, Engine Speed, and Fuel Flow for the modeled (blue) 48 V P0 MHEV and tested (red) 115 V P0 MHEV (Malibu Eco) over the UDDS

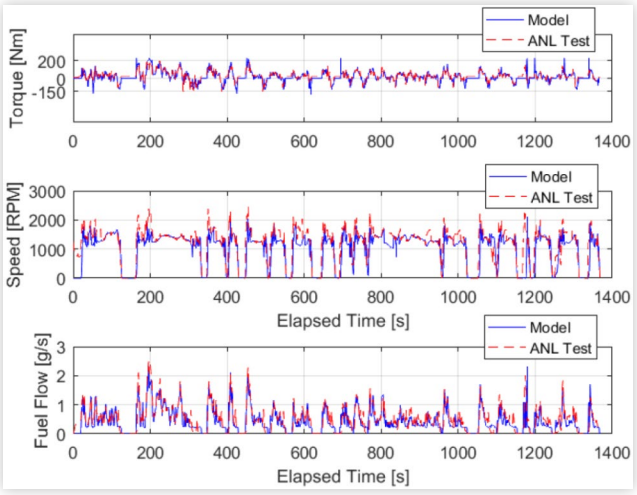

FIGURE 15 Comparison of Transmission Gear Selection Data for the Modeled 48 V P0 MHEV and Measured P0 115 V MHEV (top) Relative to Pedal Acceleration and Vehicle Speed (Bottom) over the UDDS

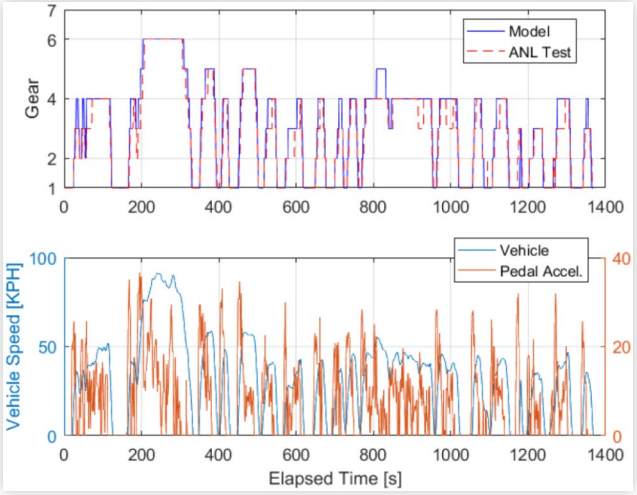

HwFET Simulations of 48 V P0 MHEV

As shown in Figure 18, engine torque and speed were operated near a high efficiency region to minimize fuel consumption

FIGURE 16 Comparison of Battery Power and Motor Speed for the Modeled 48 V P0 MHEV (blue) and Measured 115 V P0 MHEV (red) over the UDDS

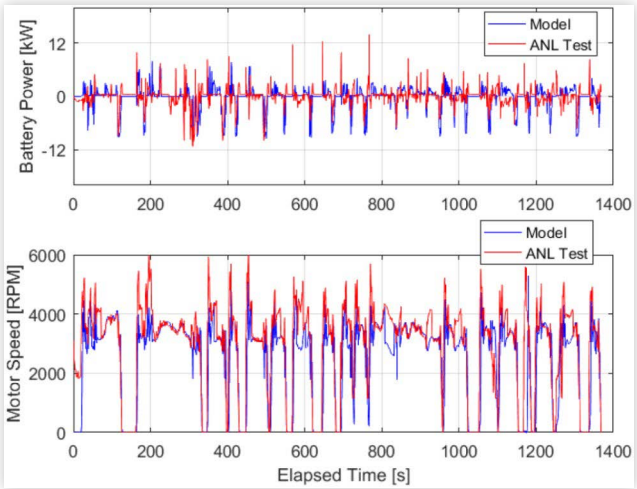

TABLE 3 - Comparison of UDDS and HwFET Fuel Economy for the 48 V and 115 V MHEVs

MHEVs	Test Cycle	Initial/Final SOC (%)	CO_2 (g/km)	Fuel Economy (mpg)	Test/Model
115 V P0 MHEV	UDDS	42/43.3	162.4	34.0	ANL Test
48 V P0 MHEV	UDDS	42/45.1	162.0	34.1	Model
115 V P0 MHEV	HWFET	43/48.3	112.9	48.9	ANL Test
48 V P0 MHEV	HWFET	43/46.7	115.4	47.9	Model

US Government / US Environmental Protection Agency

FIGURE 17 Comparison of Battery Voltage & SOC for the Modeled 48 V P0 MHEV (blue) and Measured P0 115 V MHEV (red) over the UDDS

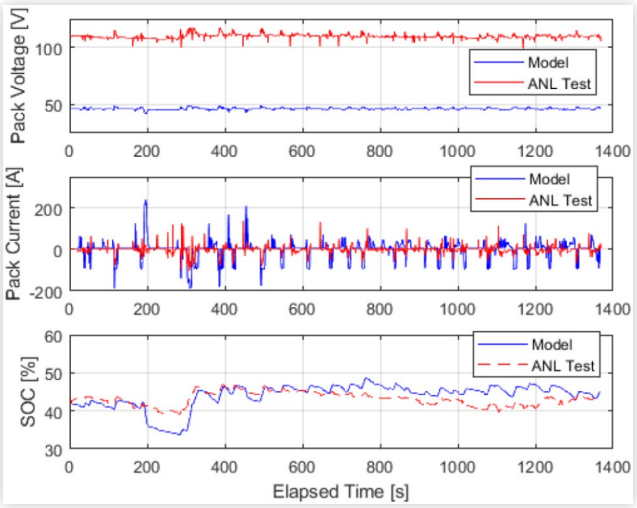

US Government / US Environmental Protection Agency

FIGURE 18 Comparison of Engine Fuel Flow for the Modeled 48 V P0 MHEV (blue) and Measured 115 V P0 MHEV (red) over the HwFET

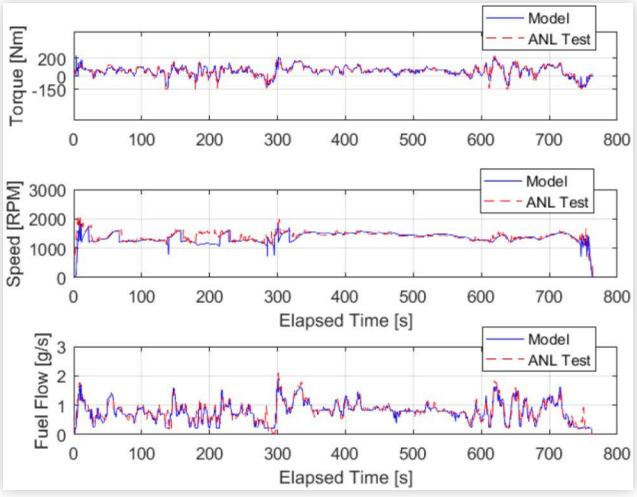

US Government / US Environmental Protection Agency

and CO_2 emissions. Excessive engine power was used to charge the battery pack when demanded engine power was low. However, demanded engine torque can be reduced to be closer to regions of high efficiency by supplying additional motor torque when the demanded driver torque exceeded the optimum engine torque. The 79.2 Nm and 11.7 kW RMS engine torque and engine power for the modeled 48 V P0 MHEV was within 2% and 0.9% of the 77.7 Nm and 11.8 kW RMS engine torque and engine power (respectively) for the 115 V MHEV chassis dynamometer test data [16]. Overall, the simulated engine torque and speed shown in Figure 18 were in good agreement with engine torque and speed from the chassis dynamometer test data.

Figure 19 shows that the transmission gear was engaged in the 6-speed position more frequently over the HwFET than for lower speed drive cycles like the UDDS. The gear selection during the 48 V model simulations was in excellent agreement with gear selection during chassis dynamometer testing of the 2013 Malibu Eco 115 V P0 MHEV.

The simulated 1.88KW RMS battery power for the 48 V P0 MHEV was within 6.0% of the 2.0 kW RMS battery power for the 115 V MHEV test data over the HwFET [16]. Overall, the simulated battery regenerative charging power and the motor speed of the 48 V MHEV shown in Figure 20 agreed well with the regenerative charging power and motor speed observed during chassis dynamometer testing of the 115 V MHEV over the HwFET.

As shown in Figure 21, the 39.6A RMS current for the 48 V MHEV was significantly higher than the 17.7A RMS current for the 115 V MHEV test data over the HwFET due to the battery pack and system voltage change from 115 V to 48 V. The final SOC of the modeled 48 V battery pack was closer to the initial SOC and was lower than the final SOC of the 115 V battery pack from the HwFET chassis dynamometer test results, and thus the modeled 48 V MHEV modeling results are conservative from a standpoint of modeled SOC

FIGURE 19 Comparison of Transmission Gear Selection Data for the Modeled 48 V P0 MHEV and Measured P0 115 V MHEV (top) Relative to Pedal Acceleration and Vehicle Speed (Bottom) over the HwFET

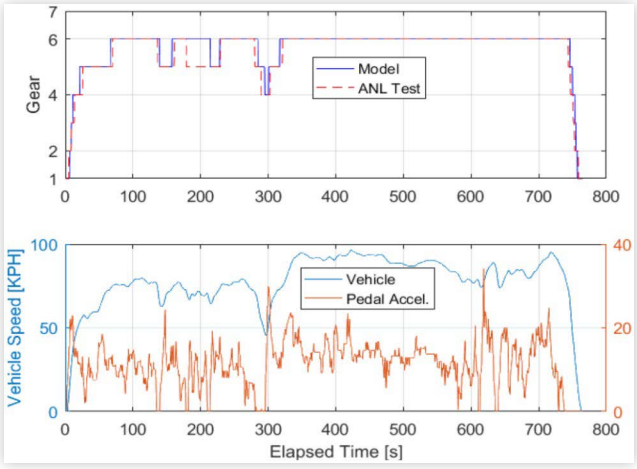

US Government / US Environmental Protection Agency

FIGURE 20 Comparison of Battery Power and Motor Speed for the Modeled 48 V P0 MHEV (blue) and Measured 115 V P0 MHEV (red) over the HwFET

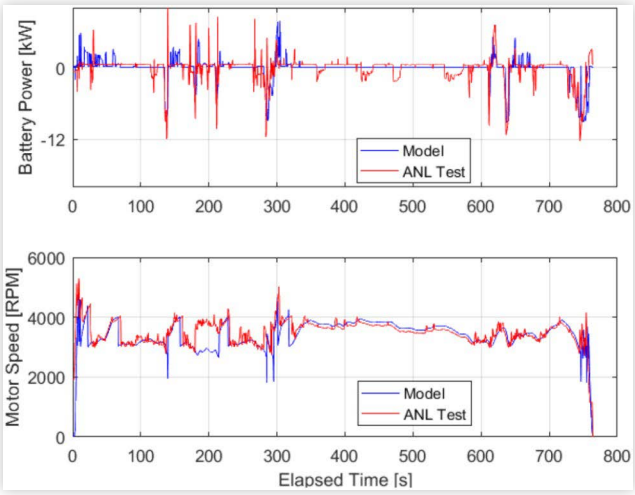

FIGURE 21 Comparison of Battery Voltage, Current & SOC for the Modeled 48 V P0 MHEV (blue) and Measured 115 V P0 MHEV (red) over the HwFET

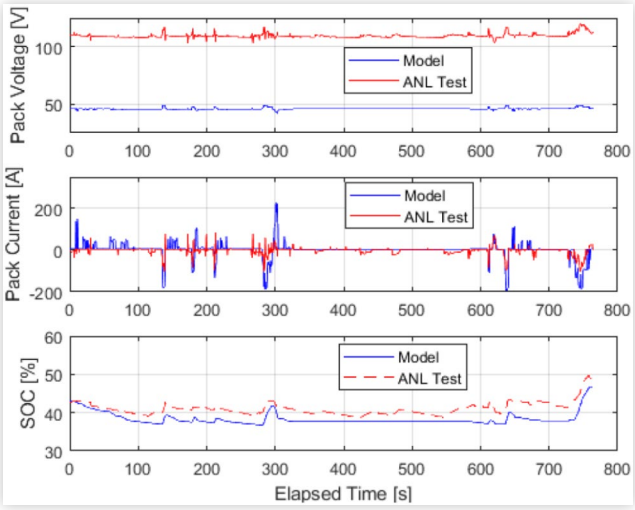

recovery over the HwFET relative to the chassis dynamometer tests.

During the HwFET, the SOC swing windows for both the modeled 48 V and the tested 115 V battery pack were smaller than over the UDDS since the engine was already operating relatively efficiently. The SOC values for both the modeled 48 V P0 MHEV and the chassis dynamometer tested 115 V P0 MHEV were within an acceptable range of the initial SOC values for valid regulatory test cycle results.

As shown in Table 3, the CO_2 and fuel economy differences between 48 V P0 MHEV model simulations and 115 V P0 MHEV test data [16] were both within 0.3% over the UDDS, and were within 2.2% and 2.0%, respectively, over the HwFET.

Conclusion

In this paper, development and validation of a 48 V MHEV model and co-simulations using 48 V Li-ion battery test data, a scaled 48 V BISG motor efficiency map, the Gamma Technology GT-DRIVE vehicle model, and vehicle component DLLs developed using EPA's ALPHA vehicle model were presented. The MHEV simulation modeled using GT-DRIVE includes a mathematical and rule-based VSC. The VSC identifies overall energy flows by controlling key parameters such as SOC, pedal acceleration/deceleration, vehicle speed, battery power limits, and driver torque demand and allows the simulation to model 48 V MHEV GHG and fuel economy on a second-by-second basis.

The 48 V MHEV P0 vehicle model was validated using 2013 Chevrolet Malibu Eco 115 V P0 MHEV chassis dynamometer test data provided by ANL. The same motor power/torque and belt pulley ratios from the 2013 Malibu Eco 115 V P0 MHEV were applied to the modeled 48 V P0 MHEV while using a 48 V/0.4kWh battery pack approximately equivalent in energy storage capacity to a 2018 Buick Lacrosse 86 V MHEV battery. Hence, the major differences between the modeled and tested vehicle configurations are the battery pack and system voltage changes. There is also an approximately 50-pound weight reduction from the 115 V pack to a smaller 48 V Li-ion battery pack, but the resultant reduction in vehicle inertia was not taken into consideration for this modeling in order to facilitate MHEV model validation with vehicle test data using the inertia of the production vehicle. Including the weight reduction may result in slightly lower GHG and improved fuel economy for the 48 V MHEV system relative to the original 115 V MHEV system. The modeled 48 V MHEV simulations showed good correlation to MHEV test data. The 48 V MHEV strategies developed for the GT-DRIVE model simulations have subsequently been integrated into EPA's ALPHA vehicle model.

Development of an HEV/MHEV model enables EPA to determine the GHG effectiveness of new advanced technologies. The model also allows estimation of the resulting fuel economy and GHG emissions obtainable via optimization of various vehicle system design variables such as vehicle weight, drag coefficient, tire friction, HEV power-coupling systems, regenerative braking efficiency, engine fuel mapping, motor efficiency, battery power and energy densities, battery SOC operating windows, battery discharge and charge power limits, BMS thermal control strategies, and other vehicle design parameters.

Modeling results for the 48 V P2 MHEV will be presented separately in the near future. High voltage P2 HEV and low voltage P2 MHEV applications share many similarities except that the 48 V MHEVs use smaller, lower torque electric machines and a lower voltage battery pack for cost-savings and weight reduction at a penalty of lower GHG effectiveness. Conserving vehicle mass to provide additional available payload is critical for the large light-duty trucks, and thus 48 V P0 and P2 MHEV systems may be well suited for such applications.

References

1. Lee, B., Lee, S., Cherry, J., Neam, A. et al., "Development of Advanced Light-Duty Powertrain and Hybrid Analysis Tool (ALPHA)," SAE Technical Paper 2013-01-0808, 2013, doi:10.4271/2013-01-0808.
2. Newman, K., Kargul, J., and Barba, D., "Benchmarking and Modeling of a Conventional Mid-Size Car Using ALPHA," SAE Technical Paper 2015-01-1140, 2015, doi:10.4271/2015-01-1140.
3. Lee, S., Lee, B., Zhang, H., Sze, C. et al., "Development of Greenhouse Gas Emissions Model for 2014-2017 Heavy- and Medium-Duty Vehicle Compliance," SAE Technical Paper 2011-01-2188, 2011, doi:10.4271/2011-01-2188.
4. U.S. Code of Federal Regulations, Title 49, Part 571, Subpart B, §571.305 "Electric-Powered Vehicles: Electrolyte Spillage and Electrical Shock Protection," https://www.ecfr.gov/, accessed 13 July 2017t.
5. Lee, S., Lee, B., McDonald, J., Sanchez, J. et al., "Modeling and Validation of Power-Split and P2 Parallel Hybrid Electric Vehicles," SAE Technical Paper 2013-01-1470, 2013, doi:10.4271/2013-01-1470.
6. Chen, Min and Rincon-Mora, G.A., "Accurate Electrical Battery Model Capable of Predicting Runtime and I-V Performance," *IEEE Transaction on Energy Conversion* 21|(2:504-511, June 2006.
7. Lee, S., Lee, B., McDonald, J., and Nam, E., "Modeling and validation of Li-ion automotive battery packs," SAE Technical Paper 2013-01-1539, 2013, doi:10.4271/2013-01-1539.
8. Lee, S., Lee, B., McDonald, J., and Safoutin, M., "HIL Development and Validation of Lithium-Ion Battery Packs," SAE Technical Paper 2014-01-1863, 2013, doi:10.4271/2014-01-1863.
9. Dekraker, P., Kargul, J., Moskalik, A., Newman, K. et al., "Fleet-Level Modeling of Real World Factors Influencing Greenhouse Gas Emission Simulation in ALPHA," *SAE Int. J. Fuels Lubr.* 10(1):e0187101, 2017, doi:10.4271/2017-01-0899.
10. Rodriguez, J., Keribar, R., and Wang, J., "A Comprehensive and Efficient Model of Belt-Drive Systems," SAE Technical Paper 2010-01-1058, 2010, doi:10.4271/2010-01-1058.
11. Kim, N., Rousseau, A., and Rask, E., "Autonomie Model Validation with Test Data for 2010 Toyota Prius," SAE Technical Paper 2012-01-1040, 2012, doi:10.4271/2012-01-1040.
12. Kuypers, M., "Application of 48 Volt for Mild Hybrid Vehicles and High-Power Loads," SAE Technical Paper 2014-01-1790, 2014, doi:10.4271/2014-01-1790.
13. Kok, D., "Power of Choice: The Role of Hybrid Vehicle Technology in Meeting Customer Expectations," *The Battery Show and Electric & Hybrid Vehicle Technology Conference*, 2014.
14. Lee, S., Cherry, J., Safoutin, M., McDonald, J. et al., "Modeling and Validation of 48 V Lithium-Ion Battery Pack," SAE Technical Paper 2018-01-0433, 2018, doi:10.4271/2018-01-0433.
15. U.S. Department of Energy - Office of Energy Efficiency and Renewable Energy - Vehicle Technology Office, "AVTA: 2013 Chevrolet Malibu HEV Testing Results," https://energy.gov/eere/vehicles/downloads/avta-2013-chevrolet-malibu-hev-testing-results, Dec 2017.
16. Argonne National Laboratory, "2013 Chevrolet Malibu Eco," from the Downloadable Dynamometer Database, http://www.anl.gov/energy-systems/group/downloadable-dynamometer-database/hybrid-electric-vehicles/2013-chevrolet, Dec 2017.
17. Burress, T., "Benchmarking of Competitive Technologies," Oak Ridge National Laboratory, Project ID: APE006, U.S. DOE Hydrogen and Fuel Cells Program and Vehicle Technologies Program Annual Merit Review and Peer Evaluation Meeting, Washington, DC, May 2012.
18. Johnson, V., Wipke, K., and Rausen, D., "HEV Control Strategy for Real-Time Optimization of Fuel Economy and Emissions," SAE Technical Paper 2000-01-1543, 2000, doi:10.4271/2000-01-1543.
19. Kum, D., Peng, H., and Bucknor, N. K., "Supervisory Control of Parallel Hybrid Electric Vehicles for Fuel and Emission Reduction," *ASME Journal of Dynamic Systems, Measurement and Control*, Apr 2010 (DS-09-1340).

Contact Information

SoDuk Lee, Ph.D.
Assessment & Standards Division
US EPA - Office of Transportation & Air Quality
734-214-4373
lee.soduk@epa.gov

Disclaimer

This document has been reviewed in accordance with U.S. Environmental Protection Agency policy and approved for publication. The views expressed by individual authors, however, are their own, and do not necessarily reflect those of the U.S. Environmental Protection Agency.

Acknowledgments

The authors would like to acknowledge the following persons for their cooperation to this model development and validation.

Kevin Stutenberg and Henning Lohse-Busch, Eric Rask, Michael J. Duoba of Argonne National Laboratory for providing chassis dynamometer test data.

Tim Burress at Oak Ridge National Laboratory for providing motor efficiency test data.

Mr. Joseph Wimmer and Ryan Tooley at Gamma Technologies for their extensive technical support with GT-DRIVE.

Definitions/Abbreviations

ALPHA - Advanced Light-Duty Powertrain and Hybrid Analysis
ANL - Argonne National Laboratory
ATDC - After top dead center
BISG - Belt integrated starter generator
BMS - Battery management system
BSFC - Brake specific fuel consumption
BTE - Brake thermal efficiency
CAD - Crankshaft angle degrees (°)
DLL - Dynamic link library
DOE - Design of experiments
EPA - Environmental Protection Agency
GDI - Gasoline direct injection
GEM - Greenhouse Gas Emissions Model
GHG - Greenhouse gas
HEV - Hybrid electric vehicle
HIL - Hardware-in-the-loop
HwFET - Highway fuel economy test procedure
LD - Light duty
MHEV - Mild hybrid electric vehicle
MTE - Midterm Evaluation
ORNL - Oak Ridge National Laboratory
PFI - Port fuel injection
PID - Proportional-integral-derivative
SOC - State of charge
TDC - Top dead center firing
UDDS - Urban dynamometer driving schedule
VSC - Vehicle supervisory control

Appendix

APPENDIX FIGURE 1 A 4-Quadrant 48 V BISG Motor Efficiency Map Derived via Scaling of Publicly Available Data

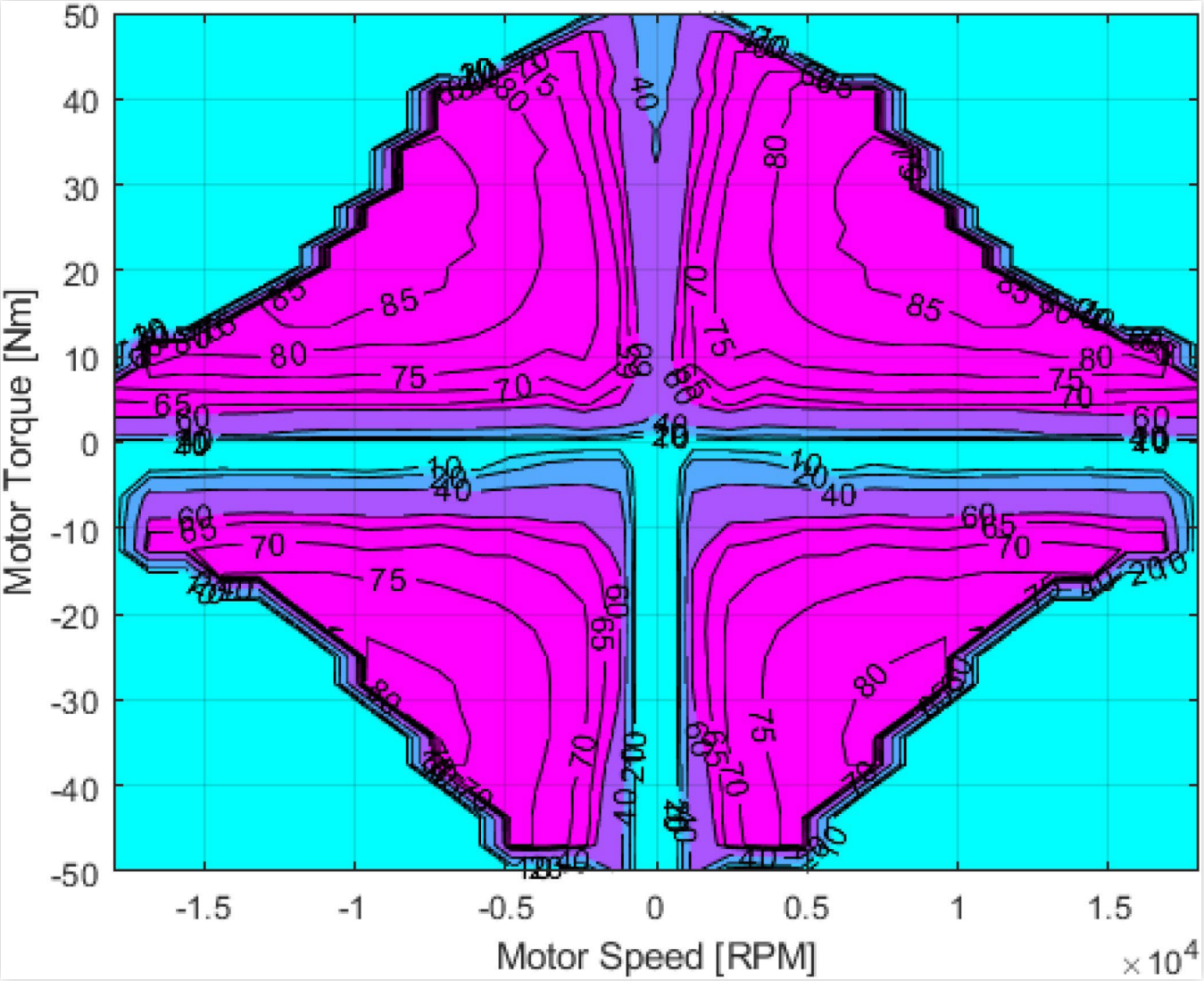

APPENDIX FIGURE 2 Schematic representation of GT-DRIVE Engine State and ALPHA Engine Model DLLs.

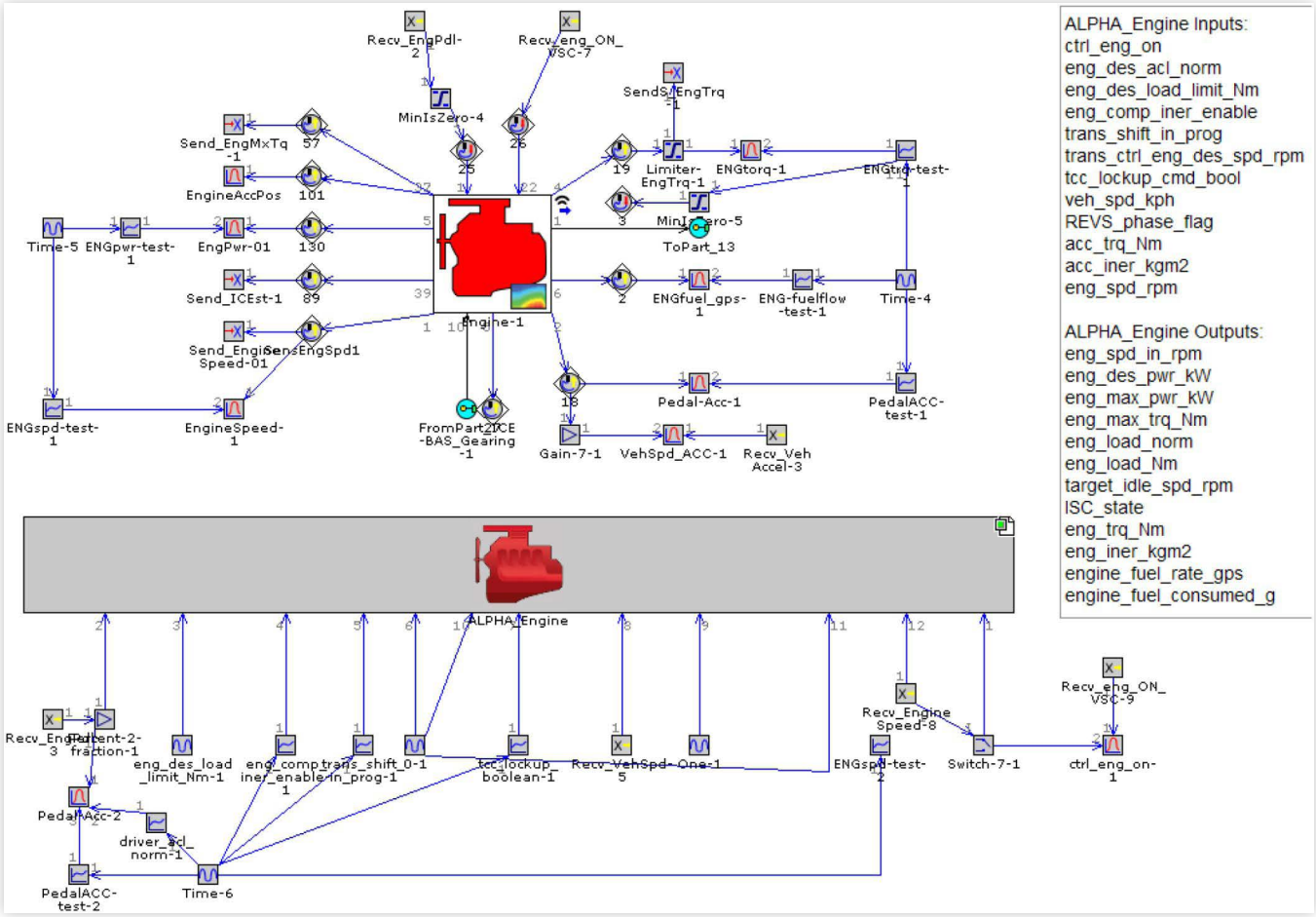

ISSN 0148-7191